

Utilization of a 3-D tissue engineered model to investigate the effects of perfusion on gynecologic cancer biology

Journal of Tissue Engineering
Volume 12: 1–14
© The Author(s) 2021
Article reuse guidelines:
sagepub.com/journals-permissions
DOI: 10.1177/20417314211055015
journals.sagepub.com/home/tej



Alba Martinez¹, Molly S Buckley², Carly B Scalise¹,
Dezhi Wang³ , Ashwini A Katre¹, Michael J Birrer⁴,
Joel L Berry² and Rebecca C Arend¹ 

Abstract

Among gynecologic malignancies, ovarian cancer (OC) has the poorest survival rate, and its clinical management remains challenging due to the high rate of recurrence and chemoresistance. Improving survival for these patients is critical, although this requires the ability to translate preclinical studies to actual patient care: bench to bedside and back. Our objective was to develop a preclinical model that accurately represents tumor biology and its microenvironment. We utilized SKOV-3, OVCAR-8, and CS-99 cell lines to show that this model was suitable for in vitro assessment of cell proliferation. We tested OC cells independently and in co-culture with cancer associated fibroblasts (CAFs) or immune cells. Additionally, we used patient-derived ovarian carcinoma and carcinosarcoma samples to show that the system maintains the histologic morphology of the primary tissue after 7 days. Moreover, we tested the response to chemotherapy using both cell lines and patient-derived tumor specimens and confirmed that cell death was significantly higher in the treated group compared to the vehicle group. Finally, we immune profiled the 3-D model containing patient tissue after several days in the bioreactor system and revealed that the immune populations are still present. Our data suggest that this model is a suitable preclinical model to aid in research that will ultimately impact the treatment of patients with gynecologic cancer.

Keywords

Ovarian cancer, gynecologic cancer, carcinosarcoma, tissue surrogates, bioreactor, personalize medicine, translational research

Date received: 20 July 2021; accepted: 6 October 2021

Introduction

Approximately 90,000 women are diagnosed with a gynecologic malignancy each year in the United States and roughly one third will experience disease-related mortality.¹ Gynecologic malignancies develop in the female reproductive system in areas including the cervix, ovary, uterus, vagina, and vulva. Ovarian cancer (OC) is the leading cause of mortality among gynecologic malignancies, and the fifth-leading cause of death in women worldwide.² Epithelial ovarian cancer (EOC) develops on the epithelium of the ovary and fallopian tubes, and accounts for nearly 90% of all OC cases.³ High grade serous ovarian cancer (HGSOC) is the most common EOC subtype and the majority of these patients will be diagnosed with advanced-stage disease associated with a 5-year survival

rate <45%.⁴ Ovarian carcinosarcoma (OCS), also known as malignant mixed mesodermal tumor or malignant mixed Müllerian tumor (MMMT), is a rare and aggressive

¹Department of Obstetrics and Gynecology, University of Alabama at Birmingham, Birmingham, AL, USA

²Department of Biomedical Engineering, University of Alabama at Birmingham, Birmingham, AL, USA

³Department of Pathology, University of Alabama at Birmingham, Birmingham, AL, USA

⁴Winthrop P. Rockefeller Cancer Institute, University of Arkansas for Medical Sciences, Little Rock, AR, USA

Corresponding author:

Rebecca C Arend, O'Neal Comprehensive Cancer Center, University of Alabama at Birmingham, 1824 6th Avenue South, WTI 430 J, Birmingham, AL 35233, USA.
Email: rarend@uabmc.edu



subtype of OC. These tumors harbor both epithelial and mesenchymal cellular components making them difficult to treat.⁵ Both HGSOC and OCS have a high rate of disease recurrence that develops from chemoresistance. Approximately 23% of patients have recurring disease within 6 months of ending chemotherapy treatment and about 60% relapse after 6 months.⁶ The development of preclinical models that recapitulate the patient's tumor microenvironment (TME) could allow for testing and identification of durable and personalized therapeutic interventions to translate into improved outcomes for these patients.

Current preclinical models for drug development consist of two-dimensional (2-D) and three-dimensional (3-D)/spheroid or organoid cultures, and murine models.⁷ While these systems provide valuable information, they have not been successful in accurately predicting the efficacy of therapies in the clinic. The limited translational potential of these models can be partially attributed to their inability to adequately mimic the patient TME. The traditional, 2-D *in vitro* models create an artificial environment that fails to replicate tumor dimensionality and an appropriate TME due to the lack of stromal components such as cancer associated fibroblasts (CAFs), extracellular matrix (ECM), and immune cells.⁸ As a result, many studies have attempted to optimize 3-D models.^{9–15} 3-D spheroid or organoid models allow for the inclusion of additional cellular components, such as fibroblasts or immune cells, that may or may not be embedded in an ECM in order to create an assay model which allows for more relevant physiological structure of the cells^{13,14,16–19} and 3D interactions between these cell types *in vivo*.^{20,21} These models can be created through spontaneous aggregation of cells *in vitro* or seeding of these cells on a substrate representing a tumor ECM.^{22,23} Even though the 3-D spheroid and organoid models allow for the co-culture of primary tumor and microenvironment cell types, these models still lack nutrient gradients, biomechanical regulation, microvascular supply, and the complete dimensionality of a TME. They also do not include the hydrodynamic pressure and forces that are present in human ovarian cancer tumors due to blood flow throughout the tumor and the presence of ascites around the ovaries. In an attempt to overcome the limitations of the 2-D and 3-D models, *in vivo* murine models have been widely used in preclinical studies. However, studies have shown significant differences in drug metabolism between mice and humans which highlights one of the many pitfalls of this preclinical model.²⁴

Previously, a 3-D microvascularized perfused bioreactor system was developed as a preclinical model for breast cancer.^{25–27} This model is unique from current 3-D models in that it includes more human cellular components such as cancer-associated fibroblasts and PBMCs, a tumor microenvironment with the appropriate ECM components, and a tumor volume that is 1cm on its longest dimension which

is the approximate size of a human tumor biopsy sample, allowing for accurate drug diffusion into the volume to accurately predict a human cancer response. By providing perfused microchannels that penetrate the 3-D matrix where cancer cells are embedded, the system overcomes diffusion limitations. In addition, the system can be customized to provide a more realistic TME with the addition of different cell types and stromal components. Overall, this 3-D perfused bioreactor provides a more accurate model of the human disease and an innovative preclinical model for personalized medicine. By using this system, we aim to develop EOC and OCS pre-clinical models that more closely mimic patient tumor biology to better predict clinical response of candidate therapies that can be translated to improve patient outcomes.

Results

Perfusion of media in bioreactor significantly increased SKOV-3 proliferation compared to solid and non-perfused systems

To determine the most efficacious system to promote EOC cell proliferation, we assessed SKOV-3 cell proliferation in solid, non-perfused, and perfused bioreactor systems (Figure 1(a) and (b)). After 7 days of culture, SKOV-3 cell density (nucleated cells/ μm^2) was significantly higher ($p < 0.001$; FC=3) in the perfused bioreactor compared to the solid and non-perfused systems (Figure 1(c) and (d)). Additionally, to test whether media perfusion had an effect on SKOV-3 biology we performed immunohistochemical (IHC) staining for PAX-8, which is used as a marker for EOC and also known to be positive on carcinomas of Müllerian origin.^{28,29} SKOV-3 cells cultured for 7 days in the perfused bioreactor were positive for PAX-8 and comparable to patient histology (Figure 1(e)). The perfused bioreactor demonstrated enhanced EOC proliferation while maintaining original patient histologic morphology.

Luciferase tagged-SKOV-3 and -OVCAR-8 cells proliferated over 7 days in the perfused bioreactor system, both independently and in co-culture with CAFs

We performed bioluminescence imaging (BLI) of *luciferase*-tagged-SKOV-3 and -OVCAR-8 (*luc*-SKOV-3 and -OVCAR-8) cells over the course of 7 days (day 0, 3, and 7) in perfused bioreactors as an independent way to objectively measure cell proliferation. We found that region of interest (ROI) radiance (Total Flux (photons/s)) from BLI matched the photomicrographs of hematoxylin and eosin-stained (H&E-stained) sections that showed an increase in cellularity over time (Supplemental Figure 1A). Cell density significantly increased (*luc*-SKOV-3, $p < 0.0001$; FC=8; *luc*-OVCAR-8, $p < 0.0001$; FC=14) over 7 days,

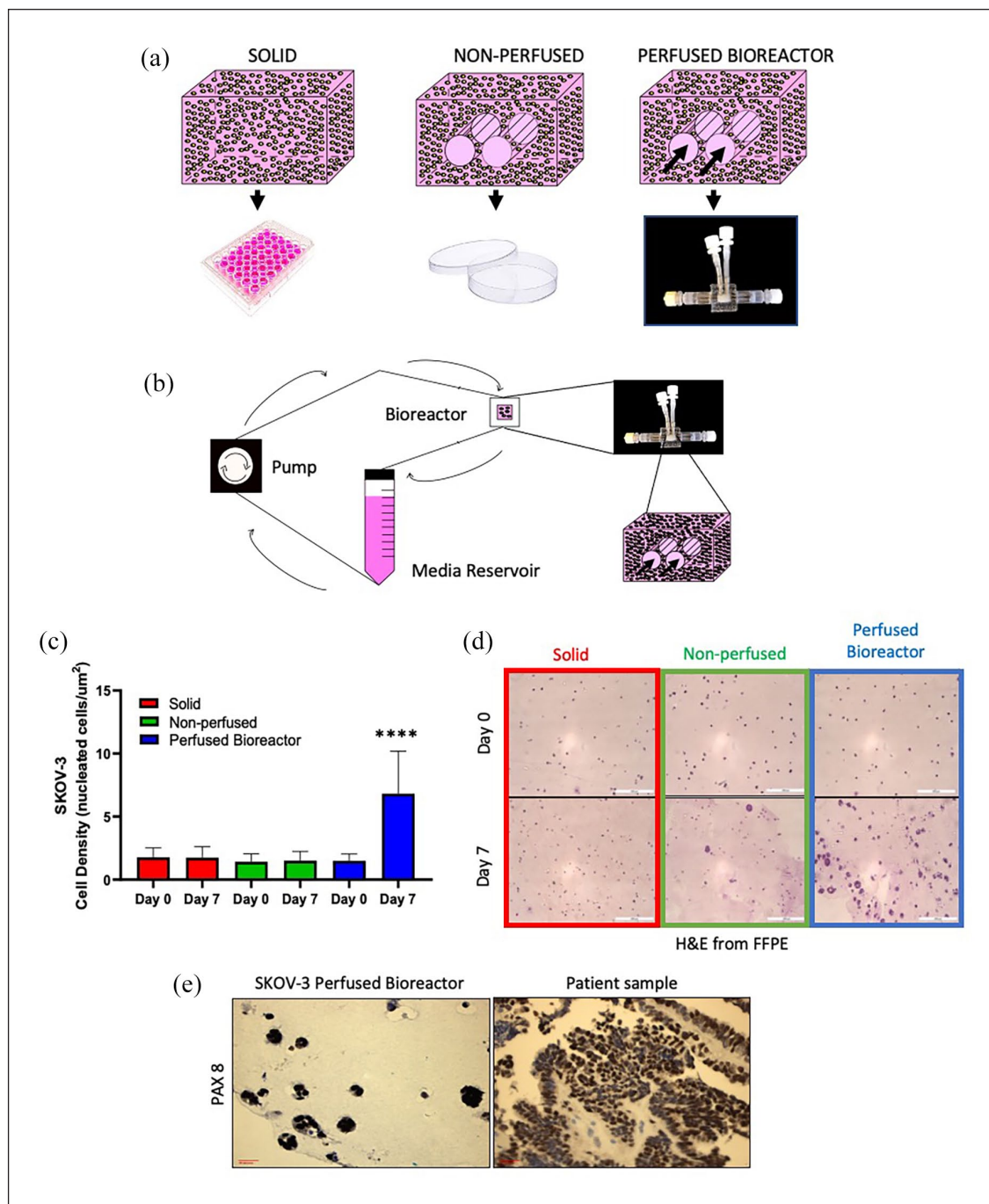


Figure 1. Perfusion of media in bioreactor significantly increased SKOV-3 proliferation compared to solid and non-perfused systems. (a) Schematic representation of the three different systems imposed on SKOV-3 cells; in all of them, the same cell concentration and matrix composition was used. (b) Schematic representation of perfused bioreactor with the flow loop consisting of pump, bioreactor, and media reservoir. (c) Cell density (nucleated cells/ μm^2) significantly increased in the perfused bioreactor after 7 days compared to the solid and the non-perfused systems. (d) Photomicrographs (200X) showed higher cellularity in the perfused bioreactor after 7 days, correlating with the cell density. (e) Photomicrographs (200X) of PAX8 immunostaining showed that the tumor cells are not modified in the perfusion bioreactor. Solid $N=3$, non-perfused $N=3$, perfused $N=6$ (*** $p < 0.0001$).

which significantly correlated with an increase in ROI radiance (*luc*-SKOV-3, $p < 0.05$, $R^2=0.969$; *luc*-OVCAR-8, $p < 0.05$, $R^2=0.995$) from BLI (Supplemental Figure 1B).

Next, we co-cultured both cell lines with CAFs, IHFOT-208 cells, at a 2:1 ratio (OC cells: CAFs). In agreement with our previous findings, there was increased ROI radiance from BLI over time and these results matched the

H&E-stained sections showing increased cellularity over time (Figure 2(a)). In addition, cell density significantly increased (*luc*-SKOV-3, $p < 0.001$; *luc*-OVCAR-8, $p < 0.001$) over 7 days and significantly correlated with ROI radiance (*luc*-SKOV-3, $p < 0.001$, $R^2 = 0.996$; *luc*-OVCAR-8, $p < 0.001$, $R^2 = 0.997$) from BLI (Figure 2(b)). Furthermore, the cell density of *luc*-SKOV-3 and -OVCAR-8 cells at day 7 was higher in perfused bioreactors with CAFs (Figure 2(b); 19.08 and 20.75, respectively) compared to those without (Supplemental Figure 1B; 8.36 and 15.50, respectively). We compared H&E-stained sections of SKOV-3:CAF tissue to tissue from a OC patient after 7 days in the perfused bioreactor and found notable similarities in histologic morphology including increased cellularity, cell shape, and spheroid formation (Figure 2(c)). These results (Figure 2) show that the culture of EOC cells independently or in co-culture had increased cell proliferation after 7 days in the perfused bioreactor. Additionally, the perfused bioreactor allowed for monitoring of cell proliferation over time using BLI, highlighting non-invasive applications of this model.

Patient-derived tumor specimens successfully maintained their histologic morphology, immune profiles, and viability after 7 days in the perfused bioreactor system

Tumor core biopsies from patients with confirmed OC diagnoses (Figure 3(a)) were collected under an IRB-approved protocol and cultured in perfused bioreactors for 7 days. Histological examination showed that tumor samples maintained their histologic morphology, via H&E stain, after 7 days in the perfused bioreactor (Figure 3(b)). Ki-67 (Figure 3(c)) and cleaved-caspase 3 (Figure 3(d)) expression were not significantly altered after 7 days of culture in the perfused bioreactor. In order to determine total cell death, a lactate dehydrogenase (LDH) assay was performed on the circulating media collected at the time of media change (day 3) and at the end of the experiment (day 7). LDH is released from cells that have structural damage via breakdown of their plasma membrane; therefore, when the cells die, LDH is released into the circulating media serving as a metabolic indicator of cell death. We found no significant difference in LDH levels over time (Figure 3(e)), confirming there was not an increase in cell death during culture in the perfused bioreactor system. These results suggest that patient-derived tumor samples maintain their cell viability with no increase in apoptosis in the perfused bioreactor.

Fresh patient tissue is a limiting factor in translational research, and methods that allow for the use of archival (frozen) patient samples are in great need. To test whether the perfused bioreactor could be used as a method to study archival patient samples, we embedded two thawed patient

specimens from our frozen tissue bio-repository into perfused bioreactors. We found that the patient sample that had been frozen for < 1 year had improved histologic morphology, via H&E stain, compared to the sample that had been frozen > 1 year (Supplemental Figure 2A). In addition, Ki-67 expression was present in the patient sample that was frozen for < 1 year, however, there was no significant change in Ki-67 expression over time (Supplemental Figure 2B). These results suggest that the perfused bioreactor is a suitable model to house both fresh and < 1 year old archival patient-derived tumor specimens for further evaluation, introducing a novel personalized medicine method with the potential to test the efficacy of therapeutic agents.

With the rise of research on immune responses in cancer, we wanted to profile the immune landscape in patient-derived specimens in the perfused bioreactor. IHC staining of markers for general immune cells (CD45⁺; Figure 4(a)), T cells (CD3⁺; Figure 4(b)), CD8⁺ cells (CD8⁺; Figure 4(c)), CD4⁺ cells (CD4⁺; Figure 4(d)), and regulatory T cells (FoxP3⁺; Figure 4(e)) revealed that the immune markers of interest were present at day 0 and there was no significant difference ($p > 0.05$) in their expression after 7 days in the perfused bioreactor. These results highlight that the patient-derived tumor samples maintain their immunologic profile in the perfused bioreactor for 7 days (CD45⁺, 0.085 vs 0.086; CD3⁺, 0.066 vs 0.072; CD8⁺, 0.038 vs 0.035; CD4⁺, 0.091 vs 0.085; FoxP3⁺, 0.031 vs 0.035). The fact that this system can keep patient tissue viable and maintain not only its intrinsic histological structure but also the immune components present in the TME, represents a major advantage for testing new therapeutics for OC, specifically immunotherapies.

Investigation of cell line and patient-derived sample tumor-intrinsic and immune responses to chemotherapy using the perfused bioreactor

Patients diagnosed with OC will typically receive chemotherapy before (neoadjuvant) or after (adjuvant) debulking surgery, and this regimen consists of a platinum- and taxol-based drug combination.³⁰ We wanted to investigate the sustainability of the perfused bioreactor in studying OC response to chemotherapy. First, we seeded *luc*-OVCAR-8 cells in co-culture with CAFs, as previously described, into the perfused bioreactor on day 0. After 5 days of culture, the circulating media was changed to media containing cisplatin (50 μ M) or paclitaxel (35 μ M) (Supplemental Figure 3A). We found a reduction in cellularity (Supplemental Figure 3B) and a significant decrease ($p < 0.0001$) in cell density (Supplemental Figure 3C) in response to treatments. This correlated to a significant decrease ($p < 0.0001$) in radiance from BLI in response to treatments (Supplemental Figure 3D and E).

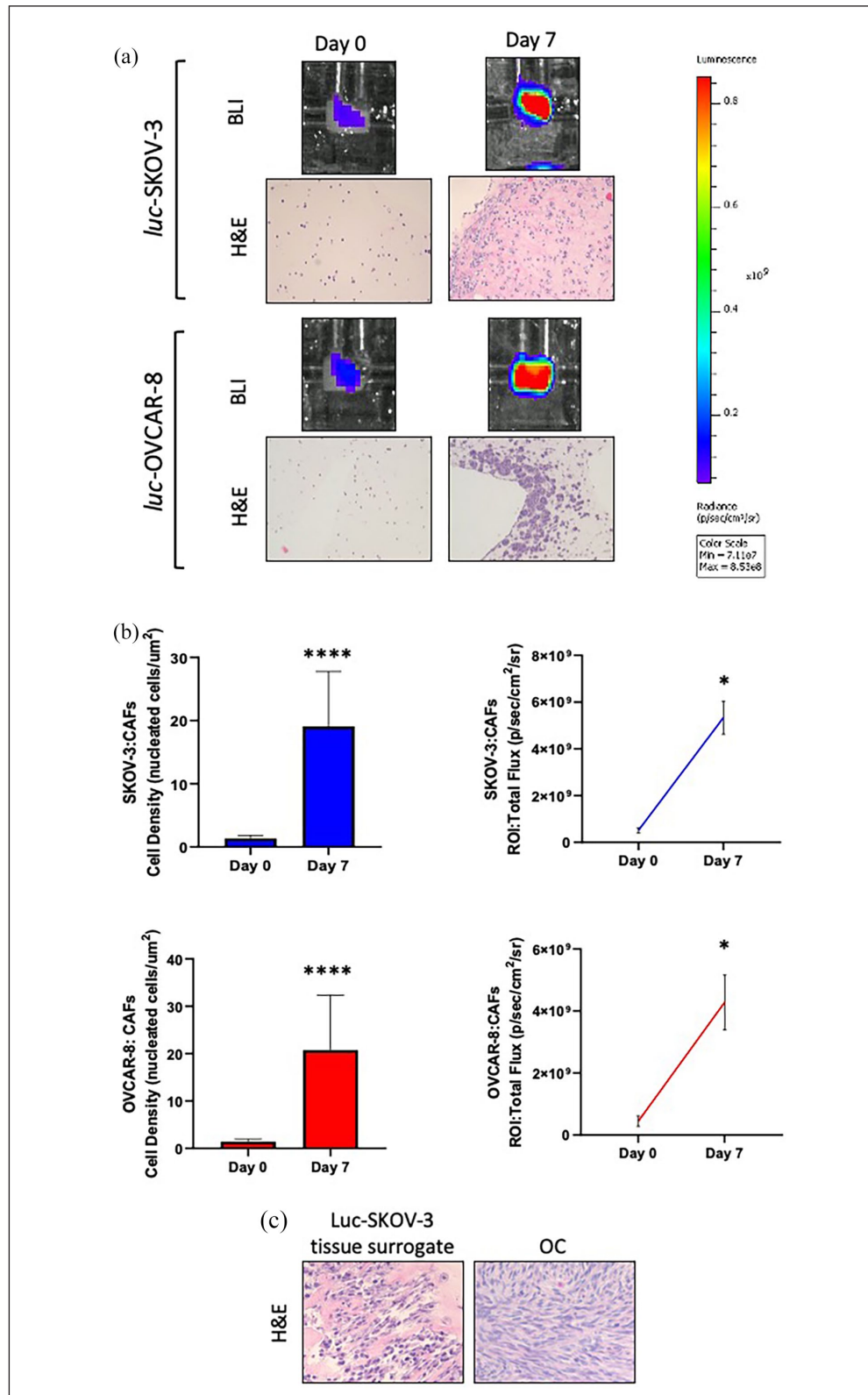


Figure 2. Co-culture of *luc-SKOV-3* and *-OVCAR-8* in the perfused bioreactor system with CAFs showed cell proliferation that is morphologically similar to patient tissue. (a) Bioluminescence imaging (BLI) and photomicrographs of H&E-stained histological sections (200X) showed increased signal and cellularity of *luc-SKOV-3* and *-OVCAR-8* cells in co-culture with IHFO2-208 (CAF) over time. (b) *SKOV-3:CAF*s and *OVCAR-8:CAF*s cell density (nucleated cells/ μm^2) showed a significant increase at day 7 versus day 0 and graphical representation of region of interest (ROI) from BLI over time was significantly higher on day 7 versus day 0. ROI positively correlated with cell density ($R^2=0.996$ and $R^2=0.997$ respectively). (c) Histology sections of co-cultured *luc-SKOV-3* and CAFs in the perfused bioreactor were morphologically similar to patient-derived tumor samples. $N=3$, **** $p < 0.0001$, * $p < 0.05$.

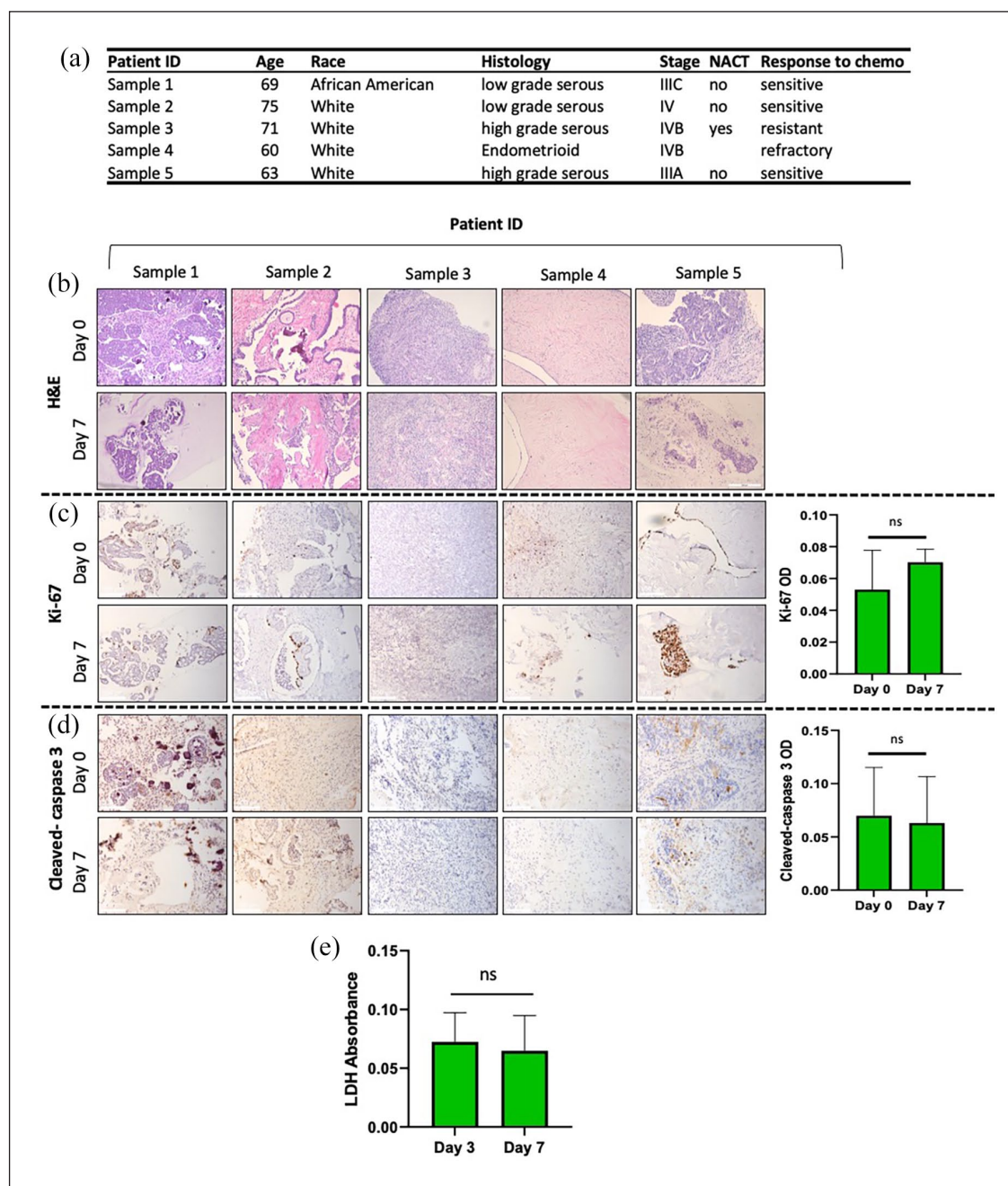


Figure 3. Patient-derived tumor specimens were successfully maintained and viable after 7 days in the perfusion bioreactor system. (a) Table of patient demographics. (b) Photomicrographs of H&E-stained histological sections (200X) showed that the tumors in the perfused bioreactors had a comparable histologic morphology with the original tumors after 7 days in the perfused bioreactor. IHC staining and Optical Density (OD) quantification showed that (c) Ki-67 and (d) cleaved-caspase 3 were present in the patient-derived bioreactor tumors but their expression did not change significantly over time. (e) Lactate dehydrogenase (LDH) analysis from the circulating media on day 3 and 7 showed no significant difference.

Next, we embedded OC patient-derived tumor samples into perfused bioreactors and treated with cisplatin and paclitaxel (chemotherapy) as previously described (Figure 5(a) and (b)). Histological examination of patient-derived tumor samples showed that after 5 days of chemotherapy, cellularity decreased (Figure 5(c)). Additionally, Ki-67

(Figure 5(d)) significantly decreased ($p < 0.05$) and cleaved-caspase 3 (Figure 5(e)) significantly increased ($p < 0.05$) in response to chemotherapy. Lastly, we found a significant increase ($p < 0.05$) in LDH in the circulating media of chemotherapy-treated bioreactors compared to controls (Figure 5(f)).

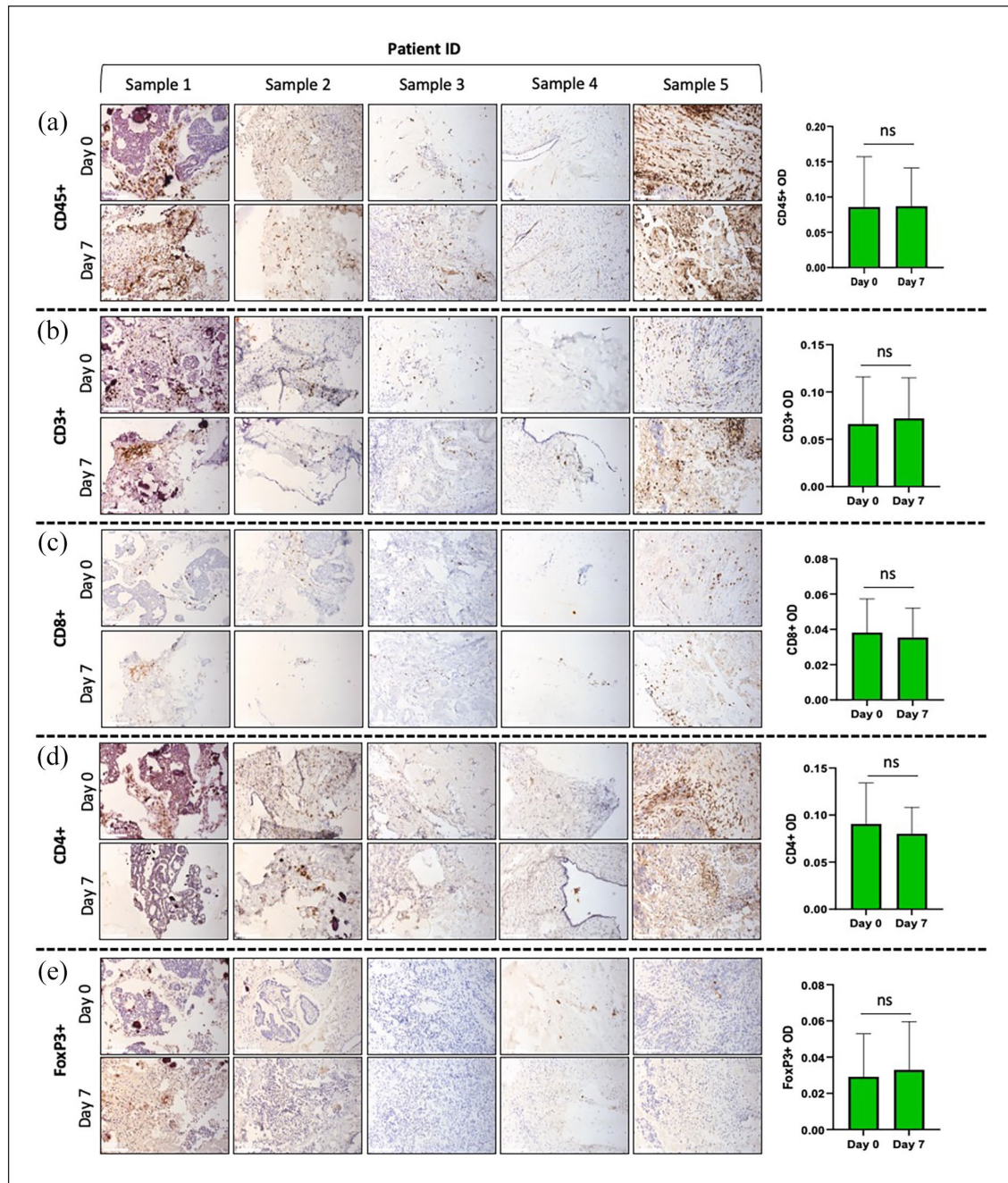


Figure 4. The immune profile of patient-derived tumors were intact after 7 days in the perfusion bioreactor system. Photomicrographs of IHC-stained histological sections (200X) and OD quantifications showed that the immune markers (a) CD45, (b) CD3, (c) CD8, (d) CD4, and (e) FoxP3 were present on the patient derived tumors cultured in the bioreactor for 7 days, but there was no significant change in their expression over time.

The effect of neoadjuvant chemotherapy (NACT) on tumor-infiltrating lymphocytes has been widely studied, and studies have shown that the density of tumor-infiltrating T cells increases after NACT.³¹ Next, we wanted to profile the T cell landscape in the patient-derived specimens that we previously treated with chemotherapy. IHC staining of markers CD4 (Figure 6(a)), CD8 (Figure 6(b)), FoxP3 (regulatory T cell marker, Figure 6(c)), and

granzyme B (cytolytic T cell marker, Figure 6(d)) were performed. We found a slight increase in CD4⁺ cells (Figure 6(a)), and a significant increase ($p < 0.05$) in CD8⁺ cells (Figure 6(b)) in response to chemotherapy. In addition, FoxP3 expression was significantly elevated ($p < 0.01$) in response to chemotherapy (Figure 6(c)), but this elevation in expression was only found in chemotherapy-resistant patient-derived samples (Figure

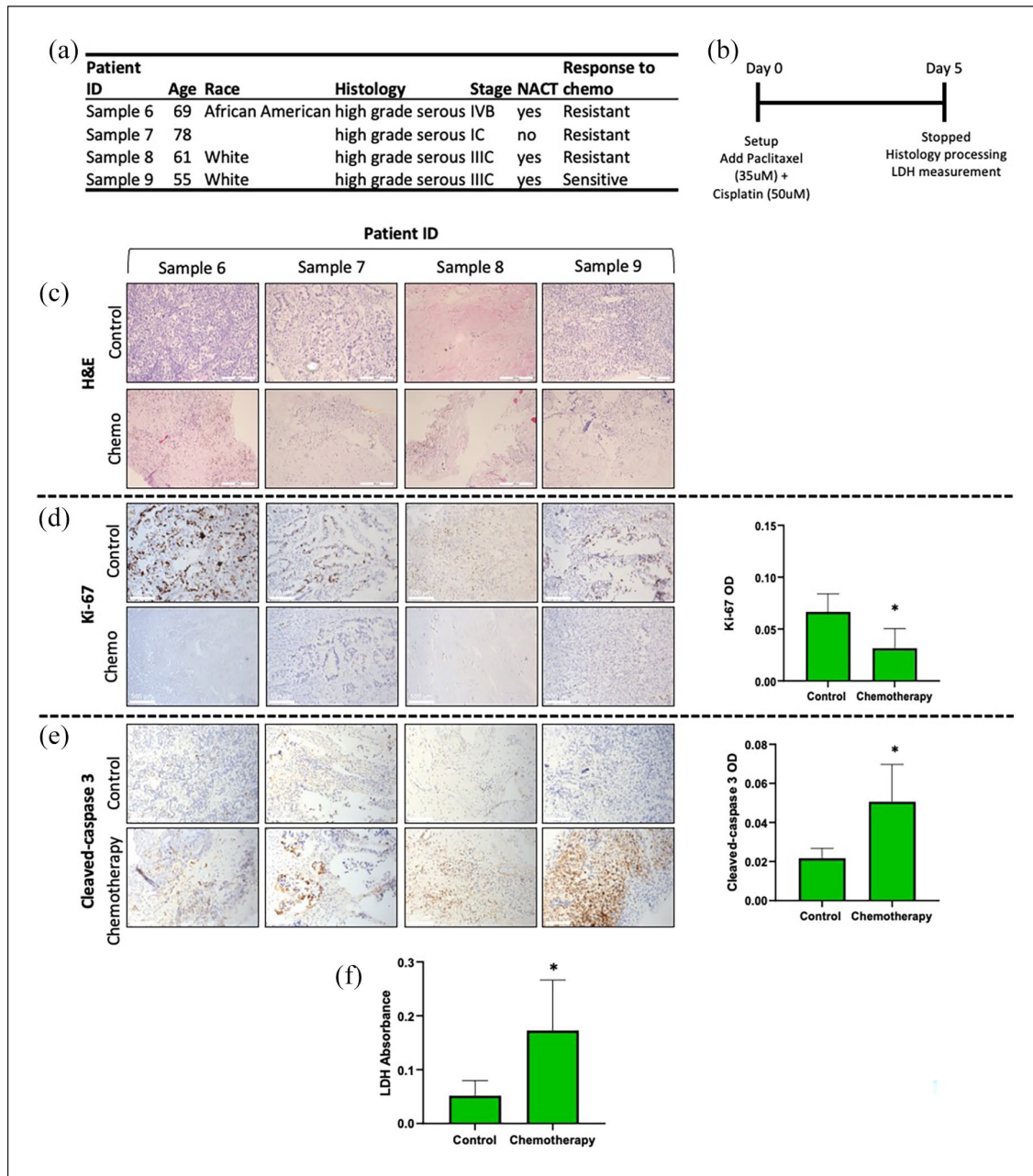


Figure 5. The perfused bioreactor system successfully supports therapeutic interventions using chemotherapy in patient-derived tumor samples. (a) Table of patient demographics. (b) Schematic of the experimental timeline. (c) Photomicrographs of H&E-stained histological sections (200X). IHC staining and OD quantification showed that (d) Ki-67 expression significantly decreased while (e) cleaved-caspase 3 significantly increased in response to chemotherapy (chemo) in the patient-derived treated tumors housed in the perfused bioreactor. (f) LDH analysis from the circulating media showed a significant difference between the control and the treated bioreactors. $*p < 0.05$.

5(a)—samples 6, 7, and 8). However, there was no significant difference in granzyme B expression in response to chemotherapy (Figure 6(d)). These data demonstrate the validity of the perfused bioreactor to study patient immune response to treatment, which is crucial given the surge in data highlighting the role of immune response in driving therapeutic efficacy.

The bioreactor system is a suitable preclinical model to study carcinosarcoma

To investigate whether the perfused bioreactor was also a suitable model for other gynecologic malignancies, we assessed the effect of Wnt modulator (DKN-01) on cell proliferation of an OCS cell line (CS-99) independently or

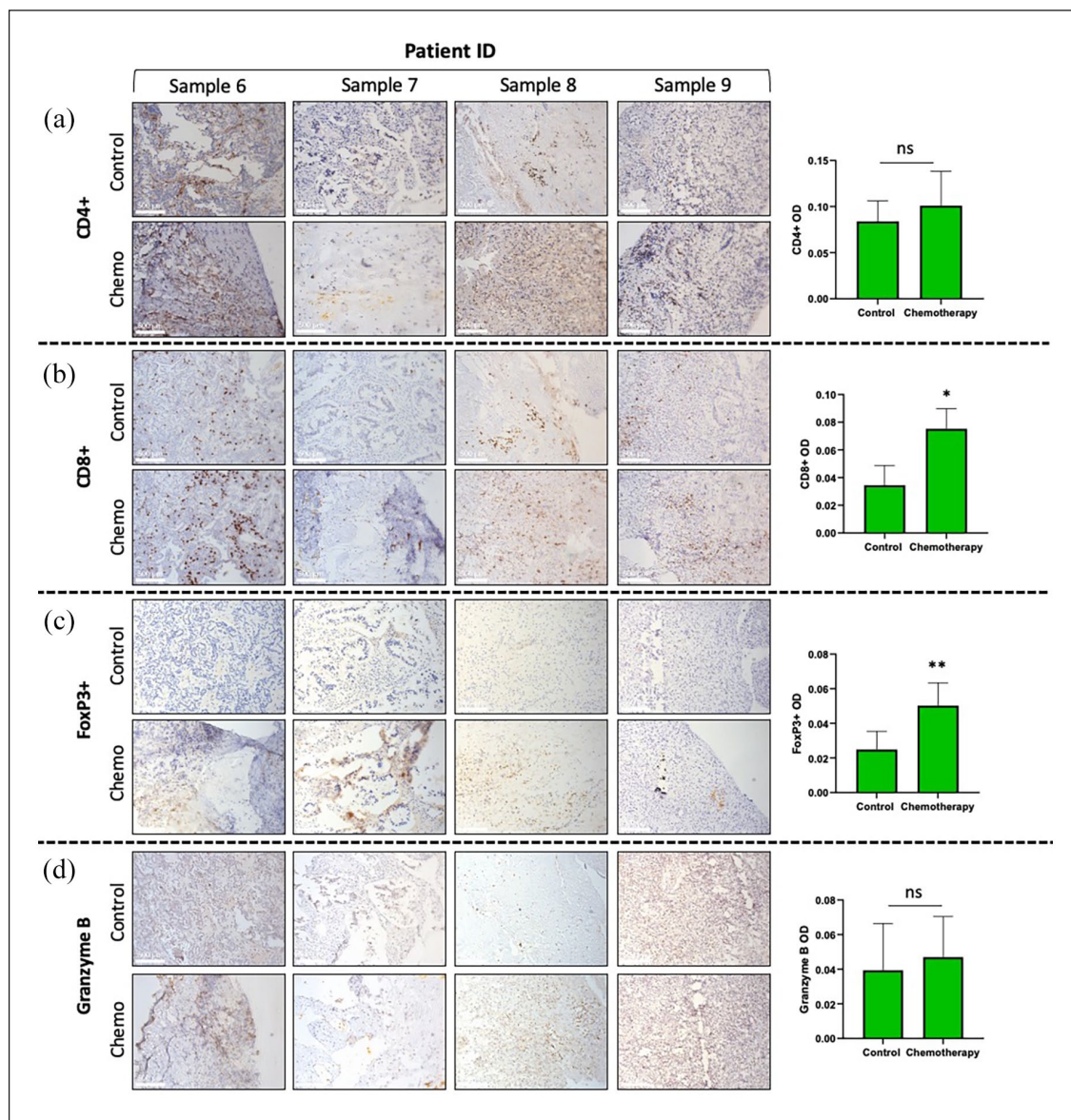


Figure 6. Chemotherapy treatment in the perfusion bioreactor system increased cytotoxic and regulatory T cells. Photomicrographs of IHC-stained histological sections (200X) and OD quantifications for immune markers (a) CD4, (b) CD8, (c) FoxP3, and (d) granzyme B showed that chemo treatment significantly increased the levels of CD8⁺ and FoxP3⁺ cells with no significant change in CD4⁺ or granzyme B⁺ cells in patient-derived tumors in the perfused bioreactors. * $p < 0.05$. ** $p < 0.01$.

in co-culture CAFs and/or peripheral blood mononuclear cells (PBMCs) (Supplemental Figure 4A). The results showed that over the course of 7 days in the perfused bioreactor CS-99 cells alone, CS-99 cells in co-culture with PBMCs, as well as CS-99 cells in co-culture with CAFs + PBMCs had increased cellularity and cell proliferation. However, treatment with DKN-01 (5 $\mu\text{g}/\text{mL}$) for 3 days decreased cellularity (Supplemental Figure 4B–D) and significantly decreased ($p < 0.0001$) cell density (Supplemental Figure 4G) compared to the control. Lastly, we tested the effects of DKN-01 on a patient-derived OCS tumor core (Supplemental Figure 4F), and similar results were observed (Supplemental Figure 4G). The co-culture

experiment with CS-99 + CAFs + PBMCs compared to CS99 cells alone brings a new layer of complexity and accuracy when recreating the TME in vitro. Overall, these results suggest that the perfused bioreactor is a suitable preclinical model to study the effects of therapeutic interventions on multiple gynecological malignancies including EOC and OCS.

Discussion

Clinical management of OC is challenging due to the high rate of recurrence and the development of chemoresistance. Unfortunately, the development and/or identification

of more durable therapeutic options has been an ineffective process,^{32,33} and one of the reasons that might contribute is the lack of preclinical models that accurately reflect a patient's TME. Currently, preclinical models for drug development rely on 2-D or 3-D cultures and murine models.⁷ Some of these models lack the complexity of cell-cell or cell-matrix interactions, tumor biomechanics, vascular architecture, and/or equivalent drug metabolism.

Here, we evaluated the perfused bioreactor for *in vitro* mono- and co-cultures as well as *ex vivo* cultures of patient-derived tumor samples. Unlike other 3-D models, the perfused bioreactor has a 3-D volume with vessel-like microchannels that allows the media to perfuse, and this perfusion significantly enhanced OC cell density compared to the solid and non-perfused systems. Moreover, the perfused bioreactor allows for non-invasive monitoring of cell proliferation using ROI radiance from BLI, which provides an extra advantage since minimal manipulation of the system is required. Furthermore, we found that the addition of CAFs and/or PBMCs increased EOC and OCS cell density compared to EOC or OCS cell culture alone, highlighting this platform as a means to study tailored co-cultures.

Importantly, the perfused bioreactor maintained patient tumor histology and cell viability without an increase in cell death in normal conditions. We also found that archival patient samples that had been frozen for <1 year could be studied in this system and had acceptable morphology and proliferation markers present. However, there was no increase in cell proliferation over time with these samples, suggesting that the addition of a cell type known to enhance proliferation (e.g. PBMCs) and/or an enrichment of the media with growth factors could be used to increase proliferation for these sample types in perfused bioreactor.

We also observed that the immune landscape of patient tumors was maintained throughout 7 days of culture in perfused bioreactors, highlighting a preclinical model that could be used to test immunotherapy options in OC. Our future directions include profiling the immune landscape of archival patient specimens to study their immune response to therapies, which would promote the applicability of this model in OC pre-clinical studies.

To provide further evidence that the perfused bioreactor could be used as a preclinical model, we evaluated the efficacy of the system to support therapeutic interventions using chemotherapeutic agents (cisplatin and paclitaxel), both in EOC cell lines and in patient-derived tumor cores. The treated tissue surrogates showed a significant decrease in cell viability with an increase in apoptosis. Also, we found that there was a significant increase in CD8⁺ cells in chemotherapy-treated bioreactors compared to the control, corresponding with previous studies.^{31,34} Expression of cytolytic T cell marker, granzyme B, did not change in response to chemotherapy. Conversely, we found a significant increase in regulatory T cell marker, FoxP3, in response to chemotherapy but this was only observed in

chemotherapy-resistant patient samples. These results suggest that the perfused bioreactor can be used to study immune response to therapies, which sets the foundation for using this model to study immunotherapy approaches. However, a limitation of this study is that we only profiled immune cells based on presence/absence and not full functionality. In the future, we will profile additional immune subpopulations and characterize their functional state in the perfused bioreactor.

Additionally, it is well understood that 7 days is not a long enough time period for a preclinical model to be used to test novel cancer drugs. The current system is not robust enough to handle prolonged perfusion without leaks or contamination. To alleviate this issue, advancements have been made to the bioreactor system. A 3-D printed bioreactor that holds the same volume of a tumor model and is one compact piece is in development. This new revision has fewer connections thus fewer opportunities for leaks or contamination of the tumor model. The ability to run these bioreactors for 14 days, 21 days, or even longer will be imperative before we will be able to move forward with this technology as a new drug development assay.

In summary, the perfused bioreactor system is suitable for (1) mono- and co-cultures of OC cells with CAFs and/or PBMCs, (2) fresh patient, and (3) <1-year archival OC patient-derived tumor samples. The utilization of archival samples in this system is important especially because fresh tissue is not always available.

Conclusion

This study aimed to investigate a novel 3-D perfused bioreactor as a preclinical model to study EOC and OCS biology and response to therapies. The main advantage of the system is that it can be customized to more accurately represent the patient TME by co-culturing different cell types and maintaining the immune landscape in patient-derived samples. The perfusion of media showed an increase in SKOV-3, OVCAR-8, and CS-99 cellularity and cell density, and this was enhanced when co-cultured with CAFs and/or PBMCs. Additionally, we demonstrated that the perfused bioreactor maintained viable tumor cores for 7 days and that histologic morphology and immune profiles were maintained. Significantly, treatment of the cancer cells or the patient-derived tumor cores with chemo- or targeted therapies resulted in increased cell death and CD8⁺ cells, providing evidence that this model is an optimal preclinical model to study immune responses that utilize patient tissue rather than a syngeneic cell model.

Materials and methods

Cell culture

The luciferase-tagged SKOV-3 ovarian cancer cell line and the CAFs cell line Human ovarian cancer fibroblast

IHFOT-208 were provided by Dr. Michael Birrer (University of Arkansas). The OVCAR-8 cell line was provided by Dr. Geeta Mehta (University of Michigan). The OVCAR-8 cell line was tagged with luciferase using retroviral infection with Firefly Luciferase Lentivirus Puromycin (Amsbio, MA). Luciferase-tagged SKOV-3 and OVCAR-8 cells were cultured in RPMI 1640 1X medium, 10% FBS (Gibco; Waltham, MA), and 1% penicillin/streptomycin (ThermoFisher Scientific; Waltham, MA) supplements. IHFOT-208 cells were cultured with DMEM (Gibco, Waltham, MA) 1X with 4.5 g/L glucose, L-glutamine, and sodium pyruvate also supplemented with 10% FBS and 1% penicillin/streptomycin. The CS99 cell line was provided by Gloria Huang (Yale School of Medicine) and was cultured with DMEM (Gibco, Waltham, MA) 1X with 4.5 g/L glucose, L-glutamine, and sodium pyruvate also supplemented with 10% FBS and 1% penicillin/streptomycin. PBMCs were purchased from Stem Cell technologies and were stored in liquid nitrogen until they were used in co-culture with the cancer cells.

Tissue collection

Tumor tissue from patients with a confirmed cancer diagnosis was collected under an IRB approved protocol (IRB-131007005) at the University of Alabama at Birmingham. Patients were consented before surgery with a written informed consent. After collection, tumors were cut, weighed, and measured to ensure each tumor core placed in the bioreactor had the same weight and size. Tumor cores were either placed in the bioreactor or stored at -80°C in frozen media (9:1 FBS:DMSO). When tumors were thawed, cores were placed in complete media that was previously warmed until the tumor cores were completely thawed and then were placed in the bioreactor with the surrounding matrix.

Bioreactor preparation

Luciferase-tagged SKOV-3, OVCAR-8, or CS-99 (5.25×10^5 total cells/100 μL ECM) with or without IHFOT-208 (2:1 cancer cell to fibroblast ratio) and/or PBMC (1.5×10^6 cells) were mixed into an ECM containing 90% bovine collagen type I (Advanced Biomatrix) + 10% basement membrane (growth factor reduced Matrigel (BM), Corning) and injected into a polydimethylsiloxane (PDMS) bioreactor (Figure 1(b)). Collagen I is used because it is abundantly found in the ovarian cancer ECM³⁵⁻³⁸ and the Matrigel is added to stabilize the collagen and act as a basement membrane. Alternatively, ovarian tumor tissue cores (approximately 0.250 g) were placed into the PDMS bioreactor and an ECM containing the above mentioned components was injected around the tumor core. In both cases, the ECM volume was perforated by two stainless steel wires and the bioreactor was placed in the incubator (37°C , 5% CO_2) for

polymerization. Next, the wires were removed, revealing two channels in the ECM/cell mixture. The bioreactors were connected to a micro-peristaltic pump and a media reservoir via peroxide cured silicone tubing (Cole Parmer), as previously described,^{26,27} and continuously perfused with 15 mL medium (RPMI 1640 1X medium, 10% FBS, 1% penicillin/streptomycin, and 1% Gentamicin) for 3–7 days while incubated (37°C , 5% CO_2), with medium changed every 3 days.

Solid, non-perfused, and perfused systems preparation

In the three different scenarios (Figure 1(a)), the same number of SKOV-3 cells (5.25×10^5 total cells/100 μL ECM) and the same matrix composition as described before (90% Collagen Type I and 10% Matrigel) was used. In the solid system, the matrix containing the cells was injected in a 48 well plate, allowed to polymerize, and media was added on top of the matrix. In the non-perfused system, the matrix containing the cells was injected in a PDMS scaffold, allowed to polymerize, and was placed in a culture plate with media covering the channels, but the media remained static, without flow. In the perfused condition (bioreactor), the matrix containing the cells was injected into a PDMS scaffold, allowed to polymerize, and was connected to the pump-flow system (Figure 1(b)).

IVIS imaging

An IVIS Lumina III imaging system was used for non-invasive bioluminescence imaging (BLI) of the bioreactors. The bioreactors were disconnected from the flow loop and BLI signal of luciferase positive cells was imaged following injection of 1 mL d-luciferin (XenoLight D-Luciferin Potassium Salt, Perkin Elmer, 5 $\mu\text{g}/\text{mL}$). Identical square regions of interest (ROI) were drawn to measure BLI signals and determine ROI size.

Histologic processing and immunohistochemistry

Following growth, the bioreactor matrix was fixed with neutral buffered formalin, processed to paraffin, and histological sections were prepared. Sections were stained with hematoxylin and eosin (H&E) to evaluate cellular morphology and cell density (number of cells per cross-sectional area). For immunohistochemical staining, serial sections 5 μm thick were cut from the formalin fixed, paraffin embedded tissue blocks and floated onto gelatin coated charged glass slides (Super-Frost Plus, Fisher Scientific, Pittsburgh, PA), and dried overnight at 60°C . All sections for immunohistochemistry were dewaxed and stained on the automated immunostainers including Leica BOND, Leica BOND Rx, or Roche Ventana.

The markers of interest include: anti-PAX-8 (1:100, biocare clone BC12), anti-Ki-67 (1:100, ab15580), anti-CD3, mouse monoclonal, cat#PA0122 (Ready-to-Use), Leica, stained with Leica BOND autostainer (antigen retrieval with ER2 solution, 20 min); anti-CD4, mouse monoclonal, cat#PA0427 (Ready-to-Use), Leica, stained with Leica BOND autostainer (antigen retrieval with ER2 solution, 20 min); anti-CD45, mouse monoclonal, cat#PA0042 (Ready-to-Use), Leica, stained with Leica BOND autostainer (antigen retrieval with ER2 solution, 5 min); anti-CD8, rabbit monoclonal, cat#790-4460 (Ready-to-Use), Roche, stained with Roche Ventana autostainer (antigen retrieval with CC1 solution, 64 min); anti-granzyme B, rabbit polyclonal, cat#790-4283 (Ready-to-Use), Roche, stained with Roche Ventana autostainer (antigen retrieval with CC1 solution, 64 min); anti-Foxp3, mouse monoclonal [236A/E7], cat#ab20034 (1:200), Abcam, stained with Leica BOND Rx autostainer (antigen retrieval with ER1 solution, 10 min); anti-Cleaved Caspase-3, rabbit monoclonal [Asp175] (D3E9), cat#9579 (1:150), Cell Signaling, stained with Leica BOND Rx autostainer (antigen retrieval with ER1 solution, 10 min). The detection system from Leica or Roche was applied to the staining of the antibodies on their corresponding automated IHC stainers.

Cell density

Nucleated cells from the H&E-stained sections were counted across the tissue cross-section and the area (μm^2) was measured both using Image J software. The cell density was calculated using the number of nucleated cells/area (μm^2).

Chemotherapy treatment

Paclitaxel (Hospira, Inc.) and/or cisplatin (APP Fresenius Kabi USA) were diluted in 15 mL of media (RPMI 1640 1X medium, 10% FBS, 1% penicillin/streptomycin, and 1% Gentamicin) to a 35 or 50 μM concentration for paclitaxel and cisplatin respectively (five times the IC₅₀ found in 2D culture of OVCAR-8). DKN-01 (Leap Therapeutics) was also diluted in 15 mL of media to a 25 $\mu\text{L}/\text{mL}$ concentration. The medium containing the therapeutic agents was added in the media reservoir and the peristaltic pump allowed for perfusion through the bioreactors.

Lactate dehydrogenase and cytotoxicity measurement

Lactate dehydrogenase (LDH) is a cytosolic enzyme present in many different cell types and is a well-defined and reliable indicator of cytotoxicity. Damage to the plasma membrane releases LDH into the surrounding cell culture media. The extracellular LDH in the condition media can

be quantified spectrophotometrically and is an indicator of cellular cytotoxicity.

LDH measurement in the condition media from the flow loop was collected 3 days post-treatment. Invitrogen™ CyQUANT™ LDH Cytotoxicity Assay was used, as directed, to measure the free LDH level in the circulating media in response to treatment or to measure the viability of the tumor cores over time (day 3 and day 7).

Statistical analysis

Each in vitro experiment was performed at least in triplicate and results were expressed as mean \pm standard error of the mean (SEM) from a representative experiment. All data were assessed for normality using Shapiro-Wilk test, and since normality was met, parametric analyses were used to detect differences between control and experimental groups. $*p < 0.05$ was considered to be statistically significant. Two-way ANOVA was used on cell density and ROI from BLI when more than one variable was analyzed (i.e. day 0, 3, 7 or control, cisplatin and paclitaxel). Unpaired *t*-test was used for cell density, ROI from BLI, LDH, or OD quantification when just two variables were studied (day 0 vs day 7, control vs chemotherapy). All statistical analyses were performed using GraphPad Prism 5.01 (GraphPad; La Jolla, CA).

Acknowledgements

The authors would like to thank the UAB Comprehensive Cancer Center Preclinical Imaging Shared Facility (grant P30CA013148 and S10 instrumentation grant 1S10OD021697) for use of IVIS Lumina III imaging system, the UAB Pathology Core Research Lab for assistance in the immunohistochemistry staining.

Declaration of conflicting interests

The author(s) declared the following potential conflicts of interest with respect to the research, authorship, and/or publication of this article: R.C.A. has participated in Advisory Boards for Leap Therapeutics, AstraZeneca, GSK, Merck, VBL Therapeutics, and Caris Life Sciences. M.J.B. serves as an advisory board member for AstraZeneca, Clovis, and GSK. The remaining authors declare no conflict of interest.

Funding

The author(s) disclosed receipt of the following financial support for the research, authorship, and/or publication of this article: This research was funded by the O'Neal Comprehensive Cancer Center and the GCS Foundation.

ORCID iDs

Dezhi Wang  <https://orcid.org/0000-0002-6265-9607>

Rebecca C Arend  <https://orcid.org/0000-0003-2108-3426>

Supplemental material

Supplemental material for this article is available online.

References

- Ledford LRC and Lockwood S. Scope and epidemiology of gynecologic cancers: an overview. *Semin Oncol Nurs* 2019; 35(2): 147–150.
- Cannistra SA. Cancer of the ovary. *N Engl J Med* 2004; 351: 2519–2529.
- Rosen DG, Yang G, Liu G, et al. Ovarian cancer: pathology, biology, and disease models. *Front Biosci* 2009; 14: 2089–2102.
- Stratton JF, Pharoah P, Smith SK, et al. A systematic review and meta-analysis of family history and risk of ovarian cancer. *Br J Obstet Gynaecol* 1998; 105(5): 493–499.
- del Carmen MG, Birrer M and Schorge JO. Carcinosarcoma of the ovary: a review of the literature. *Gynecol Oncol* 2012; 125(1): 271–277.
- du Bois A, Reuss A, Pujade-Lauraine E, et al. Role of surgical outcome as prognostic factor in advanced epithelial ovarian cancer: a combined exploratory analysis of 3 prospectively randomized phase 3 multicenter trials: by the Arbeitsgemeinschaft Gynaekologische Onkologie Studiengruppe Ovarialkarzinom (AGO-OVAR) and the Groupe d'Investigateurs Nationaux Pour les Etudes des Cancers de l'Ovaire (GINECO). *Cancer* 2009; 115(6): 1234–1244.
- Dhandapani M and Goldman A. Preclinical cancer models and biomarkers for drug development: new technologies and emerging tools. *J Mol Biomark Diagn* 2017; 8(5): 356.
- Kim JB. Three-dimensional tissue culture models in cancer biology. *Semin Cancer Biol* 2005; 15(5): 365–377.
- Levanon K, Ng V, Piao HY, et al. Primary ex vivo cultures of human fallopian tube epithelium as a model for serous ovarian carcinogenesis. *Oncogene* 2010; 29(8): 1103–1113.
- Karst AM and Drapkin R. Primary culture and immortalization of human fallopian tube secretory epithelial cells. *Nat Protoc* 2012; 7(9): 1755–1764.
- Kenny HA, Krausz T, Yamada SD, et al. Use of a novel 3D culture model to elucidate the role of mesothelial cells, fibroblasts and extra-cellular matrices on adhesion and invasion of ovarian cancer cells to the omentum. *Int J Cancer* 2007; 121(7): 1463–1472.
- Khan SM, Funk HM, Thiollou S, et al. In vitro metastatic colonization of human ovarian cancer cells to the omentum. *Clin Exp Metastasis* 2010; 27(3): 185–196.
- Iwanicki MP, Davidowitz RA, Ng MR, et al. Ovarian cancer spheroids use myosin-generated force to clear the mesothelium. *Cancer Discov* 2011; 1(2): 144–157.
- Davidowitz RA, Selfors LM, Iwanicki MP, et al. Mesenchymal gene program-expressing ovarian cancer spheroids exhibit enhanced mesothelial clearance. *J Clin Invest* 2014; 124(6): 2611–2625.
- Rizvi I, Gurkan UA, Tasoglu S, et al. Flow induces epithelial-mesenchymal transition, cellular heterogeneity and biomarker modulation in 3D ovarian cancer nodules. *Proc Natl Acad Sci USA* 2013; 110(22): E1974–E1983.
- Eke I and Cordes N. Radiobiology goes 3D: how ECM and cell morphology impact on cell survival after irradiation. *Radiother Oncol* 2011; 99(3): 271–278.
- Lee JM, Mhawech-Fauceglia P, Lee N, et al. A three-dimensional microenvironment alters protein expression and chemosensitivity of epithelial ovarian cancer cells in vitro. *Lab Invest* 2013; 93(5): 528–542.
- Muranen T, Selfors LM, Worster DT, et al. Inhibition of PI3K/mTOR leads to adaptive resistance in matrix-attached cancer cells. *Cancer Cell* 2012; 21(2): 227–239.
- Tofani LB, Sousa LO, Luiz MT, et al. Generation of a three-dimensional in vitro ovarian cancer co-culture model for drug screening assays. *J Pharm Sci* 2021; 110: 2629–2636.
- Howes AL, Richardson RD, Finlay D, et al. 3-Dimensional culture systems for anti-cancer compound profiling and high-throughput screening reveal increases in EGFR inhibitor-mediated cytotoxicity compared to monolayer culture systems. *PLoS One* 2014; 9(9): e108283–e108283.
- Kobayashi H, Man S, Graham CH, et al. Acquired multicellular-mediated resistance to alkylating agents in cancer. *Proc Natl Acad Sci USA* 1993; 90(8): 3294–3298.
- Cukierman E, Pankov R and Yamada KM. Cell interactions with three-dimensional matrices. *Curr Opin Cell Biol* 2002; 14(5): 633–639.
- Kunz-Schughart LA, Freyer JP, Hofstaedter F, et al. The use of 3-D cultures for high-throughput screening: the multicellular spheroid model. *J Biomol Screen* 2004; 9(4): 273–285.
- Gengenbacher N, Singhal M and Augustin HG. Preclinical mouse solid tumour models: status quo, challenges and perspectives. *Nat Rev Cancer* 2017; 17(12): 751–765.
- Goliwas KF, Richter JR, Pruitt HC, et al. Methods to evaluate cell growth, viability, and response to treatment in a tissue engineered breast cancer model. *Sci Rep* 2017; 7(1): 14167.
- Goliwas KF, Marshall LE, Ransaw EL, et al. A recapitulative three-dimensional model of breast carcinoma requires perfusion for multi-week growth. *J Tissue Eng* 2016; 7: 2041731416660739.
- Marshall LE, Goliwas KF, Miller LM, et al. Flow-perfusion bioreactor system for engineered breast cancer surrogates to be used in preclinical testing. *J Tissue Eng Regen Med* 2017; 11(4): 1242–1250.
- Chai HJ, Ren Q, Fan Q, et al. PAX8 is a potential marker for the diagnosis of primary epithelial ovarian cancer. *Oncol Lett* 2017; 14(5): 5871–5875.
- Tong GX, Devaraj K, Hamele-Bena D, et al. Pax8: a marker for carcinoma of Müllerian origin in serous effusions. *Diagn Cytopathol* 2011; 39(8): 567–574.
- Orr B and Edwards RP. Diagnosis and treatment of ovarian cancer. *Hematol Oncol Clin North Am* 2018; 32(6): 943–964.
- Lo CS, Sanii S, Kroeger DR, et al. Neoadjuvant chemotherapy of ovarian cancer results in three patterns of tumor-infiltrating lymphocyte response with distinct implications for immunotherapy. *Clin Cancer Res* 2017; 23(4): 925–934.
- DiMasi JA, Hansen RW and Grabowski HG. The price of innovation: new estimates of drug development costs. *J Health Econ* 2003; 22(2): 151–185.
- Paul SM, Mytelka DS, Dunwiddie CT, et al. How to improve R&D productivity: the pharmaceutical industry's grand challenge. *Nat Rev Drug Discov* 2010; 9(3): 203–214.
- Leary A, Genestie C, Blanc-Durand F, et al. Neoadjuvant chemotherapy alters the balance of effector to suppressor immune cells in advanced ovarian cancer. *Cancer Immunol Immunother* 2021; 70(2): 519–531.

35. Moser TL, Pizzo SV, Bafetti LM, et al. Evidence for preferential adhesion of ovarian epithelial carcinoma cells to type I collagen mediated by the $\alpha 2\beta 1$ integrin. *Int J Cancer* 1996; 67(5): 695–701.
36. Burleson KM, Casey RC, Skubitz KM, et al. Ovarian carcinoma ascites spheroids adhere to extracellular matrix components and mesothelial cell monolayers. *Gynecol Oncol* 2004; 93(1): 170–181.
37. Shen Y, Shen R, Ge L, et al. Fibrillar type I collagen matrices enhance metastasis/invasion of ovarian epithelial cancer via $\beta 1$ integrin and PTEN signals. *Int J Gynecol Cancer* 2012; 22(8): 1316–1324.
38. Ahmed N, Riley C, Rice G, et al. Role of integrin receptors for fibronectin, collagen and laminin in the regulation of ovarian carcinoma functions in response to a matrix micro-environment. *Clin Exp Metastasis* 2005; 22(5): 391–402.